

Improvement and Modernization of Subsonic Wind Tunnels

T. Wolf*

Technical University of Darmstadt, 6100 Darmstadt, Germany

In the last two decades, the requirements on wind-tunnel testing have increased almost constantly. Consequently, new findings and developments, as well as sophisticated design rules for tunnel components, led to the fact that a lot of wind tunnels built in earlier years have become obsolete. This does not only concern data acquisition and measuring techniques but is also valid for circuit aerodynamics and flow quality. In the present article, the basic possibilities for improvement and modernization of wind tunnels which do not represent the state-of-art are discussed by using the modernization of the 3-m low-speed wind tunnel of the Technical University of Darmstadt, Germany, as an example. In this context, the design rules of the most important wind-tunnel components are reviewed and verified by the first calibration results after reoperation of the modified tunnel.

Introduction

DESPITE the fact of rapid development of computer technology and CFD, the wind tunnel is still the major tool for predicting and guaranteeing aircraft performance. Confronted with rising competition, the airplane manufacturers are forced to guarantee the flight performances of projected airplanes with very high accuracy. Because the correspondent reductions of drag have to be proven in wind-tunnel tests, the ability to do this and to guarantee even small improvements of flight performances depends strongly on the accuracy of wind-tunnel test data. Therefore, the requirements on wind-tunnel test data quality have increased significantly in the last years.

In general, the data accuracy available from wind-tunnel tests is limited by several parameters as balance accuracy, model accuracy, measuring techniques, and test section flow quality. At the present time, because of the rapid development of computer technology and measuring techniques, the limits are mostly set by an insufficient wind-tunnel flow quality and the restricted aerodynamic simulation capabilities of conventional tunnels.

These problems were clearly recognized in the past and led to the development of the cryogenic wind tunnel and to the construction of large subsonic wind tunnels with superior flow quality like the German-Dutch wind tunnel (DNW) in Europe. But because the operating costs of such large wind tunnels are so high, a major part of the development work has to be conducted in smaller and even older tunnel facilities. In doing so, one is sometimes faced with the problem that the flow quality in such tunnels does not meet today's requirements of wind-tunnel testing, and should therefore be improved.

The present article tries to make a contribution to this problem by demonstrating how the flow quality of an existing wind tunnel can be improved. Therefore, based on the experiences gained with the modernization of the 3-m low-speed wind tunnel of the Technical University of Darmstadt, the possibilities and limits for improvement and modernization of subsonic wind tunnels are pointed out and discussed.

Presented as Paper 90-1423 at the AIAA 16th Aerodynamic Ground Testing Conference, Seattle, WA, June 18–20, 1990; received June 16, 1991; revision received Sept. 25, 1991; accepted for publication Jan. 2, 1992. Copyright © 1992 by the American Institute of Aeronautics and Astronautics, Inc. All rights reserved.

Dedicated to Professor Dipl.-Ing. B. Ewald on his 60th birthday.

*Project Engineer, Department of Mechanical Engineering, Institute for Aerodynamics and Measuring Techniques, Petersenstrasse 30. Member AIAA.

Modernization of the 3-m Low-Speed Wind Tunnel of the Technical University of Darmstadt

The low-speed wind tunnel of the Technical University of Darmstadt (Fig. 1 shows the tunnel before modernization) is one of the largest university-owned wind tunnels in Germany. The tunnel, built in 1935, was one of the few wind tunnels in Germany which escaped destruction after the end of the Second World War. Until the end of the war, the tunnel was a part of the German Research Laboratory for Soaring (DFS).

After the end of the war and the readmission of aeronautical research in Germany, the tunnel was used for aeronautical research activities as well as for industrial and vehicle aerodynamics, as it is today.

In 1974 the tunnel was modernized insofar as the old 100 KW electric motor was replaced by a more powerful motor with a drive power of 300 KW (408 hp). About 1983 it was decided to modernize the tunnel once again and to modify the tunnel circuit basically in order to meet today's requirements of wind-tunnel testing. The modernization was conducted between 1985–1989 within the scope of a research project financed by the German Ministry for Research and Technology (BMFT).

Description of the Tunnel Before Modification

The original tunnel was a Göttingen-type, single-return tunnel with an open jet test section and a contraction exit diameter of 3 m. With the installed drive power of 300 KW and a contraction ratio of 4.6, a maximum jet velocity of 57 m/s was attainable according to an energy ratio of 3.75. The par-

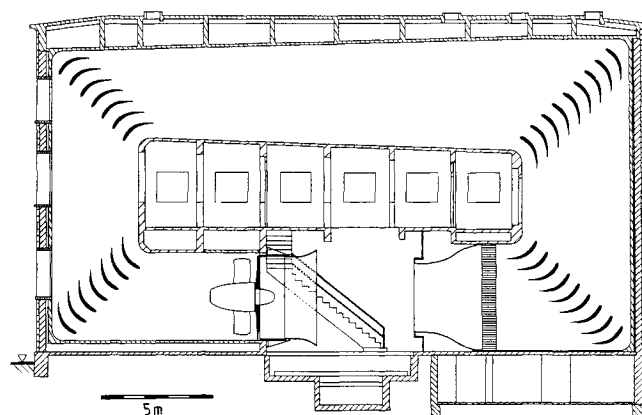


Fig. 1 3-m low-speed wind tunnel of the Technical University of Darmstadt before modernization.

ticularities of the tunnel are the vertical return duct and the thin shell made of concrete (100 mm in thickness), which is freely suspended in frames mounted in the main-tunnel building. Originally, the fan was mounted immediately downstream of the test section behind the bell-mouth and consisted of a six-blade propeller 3.8 m in diameter and five straightener vanes. Corners 1 and 2 had 7 turning vanes each, whereas corners 3 and 4 had 9 turning vanes each. The airfoil-shaped turning vanes ($c = 1.1$ m) had a relative thickness of 20%, a gap-to-chord ratio of 0.42 and a leading-edge incidence of about 4 deg. The return-leg diffuser with rectangular cross section had an area ratio of 2.11 and an equivalent cone angle of $2\theta = 7.3$ deg.

A honeycomb with a square area of 6.8×4.8 m² was installed immediately upstream of the contraction cone. To improve the test-section velocity distribution, several pieces of screens were patched directly on the upstream-side of the honeycomb. Further screens for reduction of turbulence did not exist due to the restricted space in the settling chamber. Actually, the distance between the fourth corner and the contraction inlet was so short, that in fact, no settling chamber existed.

Flow Quality of the Tunnel Before Modification

As far as known, the tunnel never suffered from unsteady flow phenomena. However, because of the open test section, the poor settling chamber design, and the absence of efficient turbulence screens, it is easy to imagine that the tunnel did not achieve a good flow quality.

Figure 2 shows the dynamic pressure distribution in the center of the open test section for a velocity of 50 m/s. Fig. 2 confirms that the test-section flow was not very uniform. There was a region of low velocity near the centerline and another region of high velocity on the upper right side of the jet. The cause for the high-velocity region was obvious, it was produced by a concrete staircase which leads to the second floor of the test section hall and was mounted directly beside the test section jet (see Fig. 1). The maximum variations of dynamic pressure from average were $\pm 4\%$ according to a velocity variation of $\pm 1.24\%$. Compared with the requirements on flow quality for today's wind-tunnel testing, these values were no longer acceptable.

The poor flow quality of the tunnel was confirmed by measurements of flow angularity and turbulence level. The flow

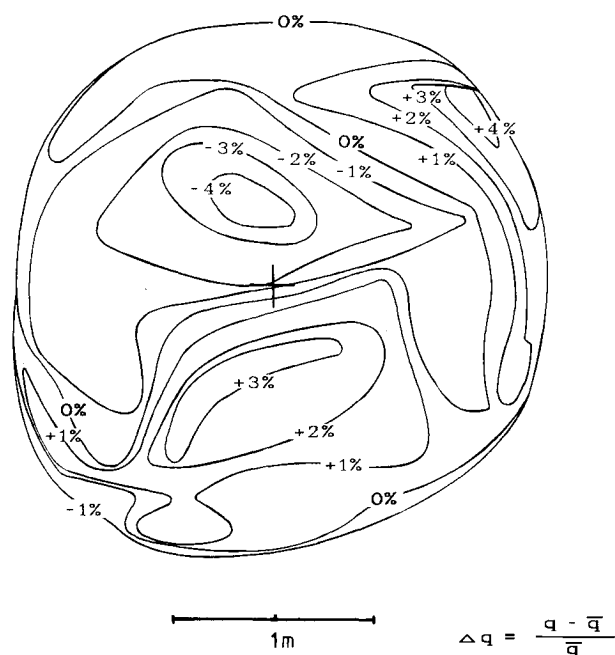


Fig. 2 Dynamic pressure variations at 50 m/s before modernization.

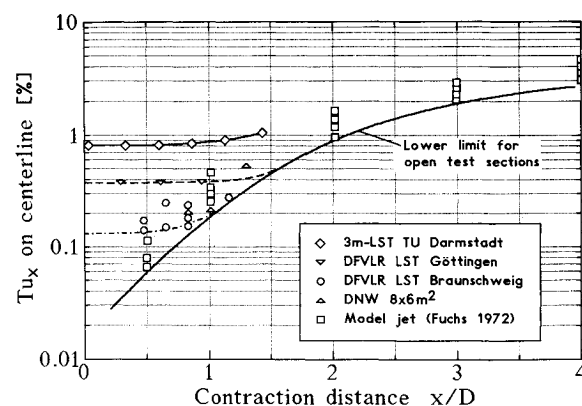


Fig. 3 Axial turbulence level at 50 m/s before modernization in comparison to the presumed lower limit for open test sections.¹

angularities covered a range of ± 1.5 deg, whereas the values for the velocity fluctuations in the axial direction measured on test section centerline were in the order of 0.75% (see Fig. 3). These turbulence values were at least twice as high as in similar tunnels and far away from the lower limit for free-jet facilities, which is assumed to be in the order of 0.15% (see Fig. 3).¹

Finally, the static pressure distribution measured along the test-section centerline showed a significantly steep pressure rise in flow direction (c.f. Fig. 12), but this is typical for most open-jet facilities.

Objects and Possibilities for Modernization

Because of the poor flow quality and the antiquated measuring and data acquisition systems, it was decided to modernize the tunnel. The objective was not only to improve the flow quality but to equip the tunnel with modern measuring techniques, data acquisition systems, and a new computer system.

To improve the flow quality of the tunnel it was proposed from the first to modify the principal aerodynamic circuit to a wide extent. For that purpose, it was projected to replace the open test section by a closed test section with a sophisticated design and to remove the fan section behind the first corner. However, to reduce the costs it was projected to use the existing drive and the existing fan without any modifications in the new tunnel. The intended circuit modifications made it quite clear that at least the tunnel components between the fourth and the second corner had to be completely redesigned.

The advantages of these modifications are obvious. With the use of a closed test section, a new fan location, a redesigned settling chamber region and contraction, a new first diffuser and new first and fourth corner, it could be expected that the flow quality in the test section would be substantially improved. In addition, the use of a modern closed test section in combination with a new external six-component platform balance would offer completely new possibilities for instruction and research.

When starting the modernization project, several possible tunnel variants were discussed. However, early investigations showed that to guarantee an optimum design of all tunnel components, the length of the basic tunnel circuit would have to be extended by at least 5–7 m. It was clear that this would increase the costs significantly and would induce technical problems and risks, because the concrete shell of the old tunnel circuit, as well as the sidewalls of the main building, would have to be broken through. Therefore, it was decided to limit the aimed modifications to the existing tunnel circuit and to modify only the tunnel sections between the fourth and the second corner. Because of the restricted space in the lower part of the tunnel circuit, an optimum design could not be realized for all tunnel components. Therefore, it was ob-

vious that even the achievable test section flow quality would probably suffer.

Conversion to a Closed Test Section

It was obvious that the intended circuit modifications would alter the aerodynamic behavior of the tunnel; i.e., the dependence between total pressure losses, mass flow, test section velocity, and the supplied motor power would change essentially. Because the existing drive should be also used in the modified tunnel, it had to be guaranteed that the fan would operate close to its original design point, but at least under the same conditions as in the old tunnel and as far as possible, with a maximum efficiency.

Therefore, the first task was to examine the conditions under which the fan was operated in the old tunnel. The investigations showed that because of various reasons, the initial design point of the fan, and especially the design value for the fan efficiency, was not totally achieved with the old tunnel configuration. The measured fan efficiency of 77.8% was about 4% lower than the design value of 82%.

The determination of the fan operating conditions which could be expected at the new fan location in the modified tunnel had to be done theoretically by calculating the total pressure losses of the new tunnel configuration. A computer program for calculating the drive power of subsonic wind tunnels was used. This program was originally developed by NASA² and has proved to be very effective in the past. For example, Fig. 4 shows the power requirements of the old tunnel calculated by the program in comparison to the measured data (note the fan efficiency of 77.8%). As can be seen, the calculated values agree very well with the measured data of the motor shaft power. Because of this good agreement it could be expected that the program would calculate the aerodynamic performance of the new tunnel configuration as well, therefore, it was used to conduct this task.

At first, the basic geometry of the new tunnel circuit had to be fixed coarsely. This was done with consideration of the corresponding design rules of each tunnel component and is described in more detail later in this article. However, it had to be guaranteed that no flow separation would occur in the diffuser sections. Therefore, the equivalent cone angle and the length of the individual tunnel sections had to be chosen appropriately. Once the basic tunnel geometry was roughly determined, the flow conditions could be calculated with the computer program mentioned above. The calculations of the fan operating conditions were carried out for several values of the test section cross-sectional area and compared with the required or desired values, respectively.

Figure 5 shows the calculated fan pressure rise for the new tunnel vs the cross-sectional area of the test section and gives information about the required operating conditions for 100 and 75% motor shaft power.³ The calculations showed that the required values for the fan operating points could be matched for a test section cross-sectional area of about 6.4

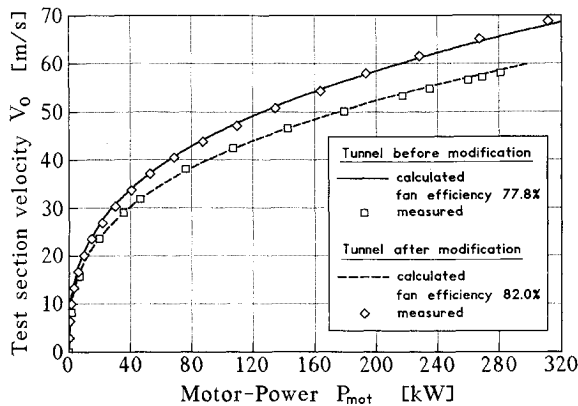


Fig. 4 Comparison of predicted and measured power requirements.

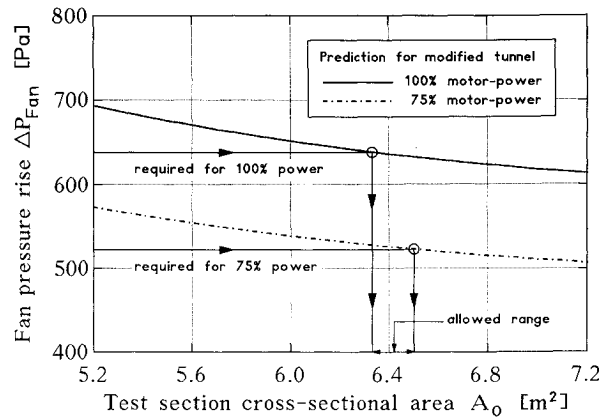


Fig. 5 Determination of the required test section cross-sectional area.

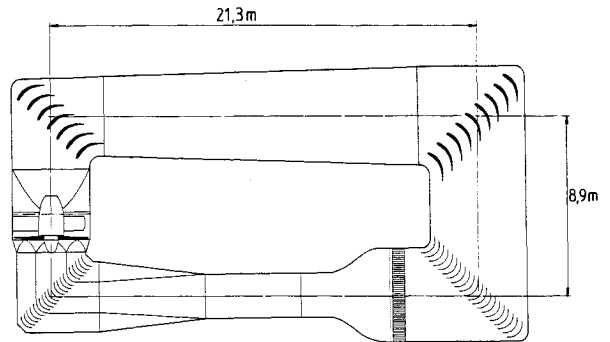


Fig. 6 Final aerodynamic circuit of the modernized $2.9 \times 2.2 \text{ m}^2$ wind tunnel.

m^2 . Therefore, according to the width-to-height ratio of 4:3 for modern test sections, a cross-sectional area of $2.9 \times 2.2 \text{ m}^2 = 6.38 \text{ m}^2$ was chosen.

Figure 6 presents the final circuit geometry of the modified tunnel which was fixed after some iterations and optimization of the individual tunnel components. As mentioned earlier, the settling chamber range was not modified despite the fact that a single turbulence screen was installed immediately downstream of the honeycomb. The new contraction behind the honeycomb ($CR = 5.2$, $L = 4.5 \text{ m}$) has a rectangular cross section and consists of 22 pieces made of composites. It is followed by the new closed test section ($L = 4.8 \text{ m}$) and the first diffuser made from wood ($L = 5.3 \text{ m}$, $AR = 1.51$, $2\theta = 7.05 \text{ deg}$), which leads to the octagonal cross section of the first corner (width across flats 3.43 m). The 21 turning vanes of the first corner as well as the new 21 turning vanes of the fourth corner are thin, unprofiled vanes made of composites. Each vane consists of a 90-deg circular arc with leading- and trailing-edge extensions of 0.1 chord length. The vanes of both corners have a gap-to-chord ratio of 0.27 and a leading-edge incidence of 0.5 deg.

The corner is followed by a transition section ($L = 0.6 \text{ m}$, $AR = 1.08$, $2\theta = 12.73 \text{ deg}$) which leads to the circular cross section of the fan duct ($L = 1.1 \text{ m}$, $D = 3.81 \text{ m}$). The fan duct itself is followed by a tail-cone diffuser transition duct ($L = 1.35$, $2\theta = 12.73 \text{ deg}$) which leads to the rectangular cross section of the unmodified part of the old tunnel circuit.

It should be mentioned here, that for the calculation of the aerodynamic performance of the new tunnel configuration, a fan efficiency of 82% was used rather than the value of 77.8% for the old tunnel version. This higher value of the fan efficiency is justified by a reduced fan tip clearance at the new fan location and was estimated by using the famous formula of Wallis⁴ as follows (average old tip clearance $s_1 = 13 \text{ mm}$, average new tip clearance $s_2 = 4 \text{ mm}$, fan blade length $L = 700 \text{ mm}$); Wallis

$$\frac{d\eta}{ds/L} = 3$$

therefore

$$\eta_2 = 0.778 + 3 \cdot [(13-3)/700] = 0.8209 \approx 82\%$$

The comparison of the calculated power requirements using a fan efficiency of 82% with the data measured after the first operation of the new tunnel is presented in Fig. 4. The calculated values agree almost exactly with the measured data. On the one hand, this confirms the reliability of the NASA program for calculating wind-tunnel power requirements but also justifies the assumptions made during the initial design phase concerning the fan efficiency. Furthermore, the results show the validity of the formula of Wallis.

Component Design and Verification of Some Design Rules

Besides the problem to guarantee the required fan operating conditions at the new fan location, the main problem of the tunnel design was to cope with the restricted space for the installation of the components which had to be redesigned and replaced as contraction, test section, first diffuser, and the transition ducts in the fan region. However, investigations in the early design period showed that the available tunnel centerline length would not be adequate to guarantee an optimum design of all tunnel components.

Because a flow separation in the first diffuser probably would have caused an oscillatory fan loading or an unsymmetrical fan inlet velocity distribution with the danger of fan surging and a reduced fan efficiency, primacy was given to the design of the first diffuser. After the diffuser length had been fixed, the remaining space was divided up for the test section and the contraction. The compromise which was chosen, using a test section length which was as small as possible, resulted in a contraction length which is essentially too short compared with the design rules known today. Therefore, it was a major task to realize a contraction contour which would guarantee an optimum flow quality at the contraction outlet and avoid any flow separation.

Design of the Diffusers

With regard to the achievable flow quality in the test section, a proper design of the diffusing sections of a wind tunnel is very important. Diffusers, especially those downstream of high-speed sections, are very sensitive to design errors which may cause flow separation. This separation can cause vibrations, oscillatory fan loadings, reduced fan efficiency, higher total pressure losses in downstream components, a distorted velocity distribution in the test section, as well as unsteady test section flow.

Therefore, the equivalent cone angle and the area ratio of a diffuser must be properly selected. Generally, to avoid flow separation, this requires that for a given area ratio the equivalent cone angle is below a certain value. For two-dimensional and conical diffusers these separation boundaries are well known, but unfortunately, for three-dimensional diffusers similar information is not available. However, in literature it is mostly recommended that the equivalent cone angle should be held 0.5–1.0 deg lower for diffusers with sharp corners than for those with a rounded cross section.² Consequently, this was the philosophy generally used for the design of the diffusing sections of the tunnel.

The above-mentioned separation boundaries for two-dimensional and conical diffusers were experimentally derived for thin inlet boundary layers. Nevertheless, calculations indicated that the boundary layers in the corners of the test section will grow very rapidly, and therefore, may be relatively thick at the inlet of the first diffuser. On the other hand it is known that the wake of a model mounted in the test section may also trigger flow separation. Therefore, especially the first diffuser was designed more conservatively resulting in a total divergence angle of about 7 deg. However, experimental investigations after the reoperation of the tunnel confirmed

that except for a small region in the corners at the diffuser inlet, no flow separation occurs, even for high-model blockages.

Design of the Contraction

As already mentioned, the limited space for installation of the new tunnel sections resulted in a contraction length which is substantially too short for the required contraction ratio of 5.2. The length of 4.5 m (which remained for the installation of the contraction after the length of the first diffuser and the test section had been fixed) is about 50% too short compared with the design rules for three-dimensional contractions known today. Hence, it was a major task during the initial design phase of the modernization project to find a contraction contour which would avoid any flow separation and guarantee optimum flow quality at the contraction outlet. Thus, it was obvious that no conventional contraction contour would come into question.

For the development of three-dimensional contractions, no reliable design rules which give information about the minimum possible contraction length are known today. However, for axisymmetric contractions it is well known that the contraction contours developed by Boerger⁵ guarantee a minimum contraction length for a prescribed flow quality at the contraction outlet under avoidance of any flow separation. The characteristics of these contractions are a cup-shaped contour with a slight area expansion in the outlet region.

For three-dimensional contractions with square or rectangular cross sections, no design method similar to that of Boerger exists. One possible way to cope with that problem is to determine the axisymmetric Boerger-contraction for the given contraction ratio and to convert it to a rectangular contraction with the same area distribution and the same length as the axisymmetric Boerger-contraction.

It is known that the problem of flow separation is much more severe for rectangular contractions because of the three-dimensional boundary-layer flow in the corners. For example, Schilawa⁶ could show by boundary-layer calculations, that for the same contraction ratio, rectangular contractions have to be at least 30% longer than axisymmetric Boerger-contractions in order to avoid boundary-layer separation in the corners. Using the minimum length of 5.15 m for an axisymmetric Boerger-contraction with the required area ratio of 5.2, this would have resulted in a total contraction length of 6.7 m which is in fact 50% more than the available space of 4.5 m. Moreover, this means that the new rectangular contraction is even shorter than an axisymmetric Boerger-contraction with the same contraction ratio.

However, there was no choice and the contraction was designed with the method described above. For this purpose, a computer program was applied which was originally developed by the National Aerospace Laboratory of The Netherlands (NLR)⁷ and was also used for the design of the various contractions of the DNW.

The program generates the contour of the desired rectangular contraction as described above or may alternatively generate any desired contraction contour. Subsequently, the flowfield through the contraction can be calculated by a finite-difference method for the solution of the potential equation. A control of the boundary-layer development is also possible by an integrated two-dimensional boundary-layer method. Figure 7 shows the computational grid and the contraction contour which was designed with the NLR-method for the contraction of the modernized wind tunnel of the TU Darmstadt.

As mentioned above, it should be noted that the contraction contour shown in Fig. 7 is not identical to the contour of a three-dimensional contraction with the equivalent area distribution of the axisymmetric Boerger-contraction, because realized rectangular contraction is 0.65 m shorter compared to an axisymmetric Boerger-contraction. Additionally, the radius of curvature in the throat of the contraction was increased

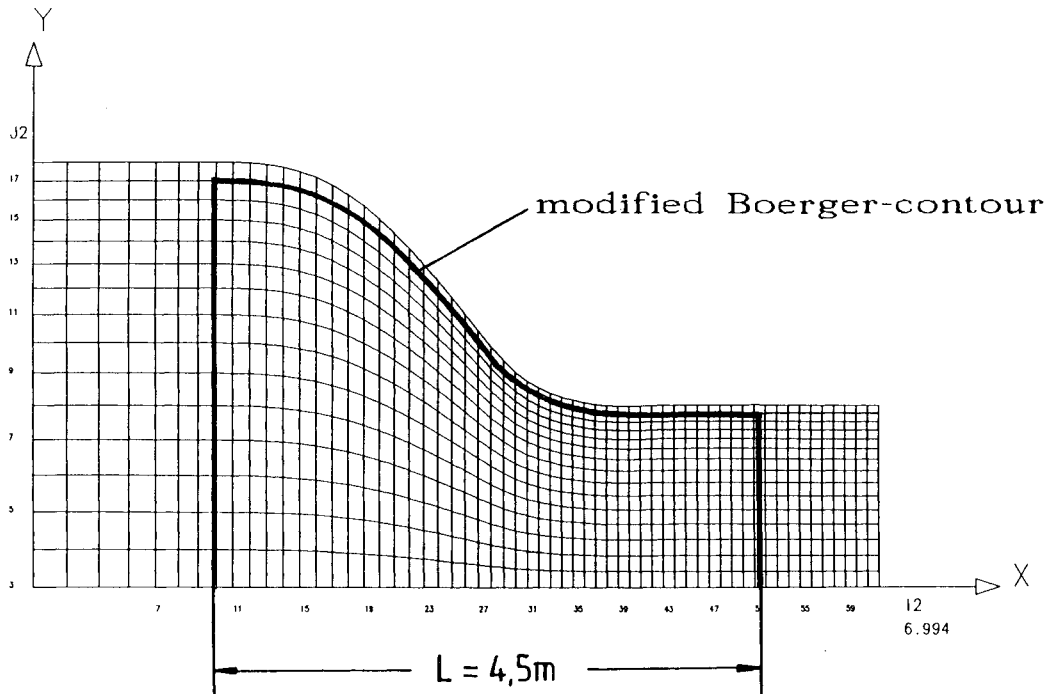


Fig. 7 Computational grid and side-wall contour of the new contraction for the $2.9 \times 2.2 \text{ m}^2$ tunnel.

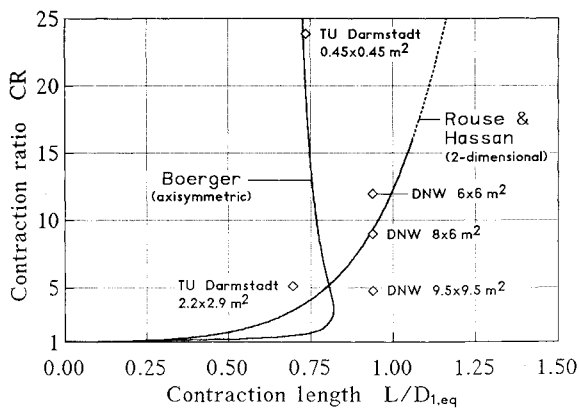


Fig. 8 Separation boundaries for axisymmetric and two-dimensional contractions.

in order to minimize the danger of a separation in the outlet region of the contraction. As expected, boundary-layer calculations indicated that this causes a higher risk for a separation near the inlet section. However, immediately downstream of the contraction inlet a single turbulence screen is installed, and it is known that screens serve to re-energize the boundary layer and reduce its thickness.⁸ Therefore, it could be expected that no separation would occur.

Figure 8 presents the comparison of several contraction designs with the separation boundaries for axisymmetric and two-dimensional contractions which was derived experimentally by Rouse and Hassan.⁹ All contractions shown in Fig. 8 are three-dimensional Boerger-contractions with rectangular or square cross sections and have been designed with the NLR-method described above.

As can be learned from Fig. 8, all contractions designed for the DNW are on the right side of the separation curve in a region, where no flow separation should occur, whereas both contractions of the TU Darmstadt are left of the limiting curve in a region where separation could probably occur. However, the newly-designed contraction of the modernized $2.9 \times 2.2 \text{ m}^2$ tunnel is close to the separation curve, whereas the Boerger-contraction of the $0.45 \times 0.45 \text{ m}^2$ nonreturn low-

speed tunnel of the TU Darmstadt exceeds the separation boundary severely.

As is well known none of the DNW contractions did ever suffer from flow separation. But the experimental investigation of the contraction of the nonreturn wind tunnel of the TU Darmstadt ($CR = 24$) revealed flow separation in all four corners near the throat of the contraction. In contrast to this, the experimental investigation of the new contraction of the $2.2 \times 2.9 \text{ m}^2$ tunnel gave no hints for any flow separation, neither in the inlet region nor in the outlet region.

Therefore, it can be concluded that the separation boundary of Rouse and Hassan seems to be a good approximation for even three-dimensional contractions. Nevertheless, further experimental investigations are necessary, especially for very high contraction ratios.

Design of the Settling Chamber

Because of the difficult accessibility and the too-short length of the settling chamber, it was clear from the beginning that an optimum configuration with several turbulence screens could hardly be realized. Therefore, it was decided to retain the existing honeycomb and to install only one turbulence screen.

It is well known that honeycombs alone reduce lateral turbulence more than axial turbulence, whereas screens alone reduce axial turbulence more than the lateral turbulence. The disadvantage of honeycombs is that they generate new turbulence in their wake which decreases slower than the disturbances produced by screens. Therefore it has been proposed to install a turbulence screen immediately downstream of the honeycomb.

For an optimum configuration it is suggested to use a honeycomb with a relative length of $L/M \geq 8-10$ (M is the honeycomb mesh size), and to install a fine turbulence screen within a relative distance of $x/M \leq 5$ immediately downstream of the honeycomb.¹⁰ These recommendations are confirmed by the experimental investigations of Scheiman and Brooks.¹¹ Moreover, they found that a combination of a honeycomb and a single screen reduces the axial turbulence even better than the screen alone.

According to Scheiman and Brooks, a combination of a honeycomb and a single screen is as fully effective as the configuration of three corresponding single screens in reducing axial turbulence. Based on these findings, it was decided

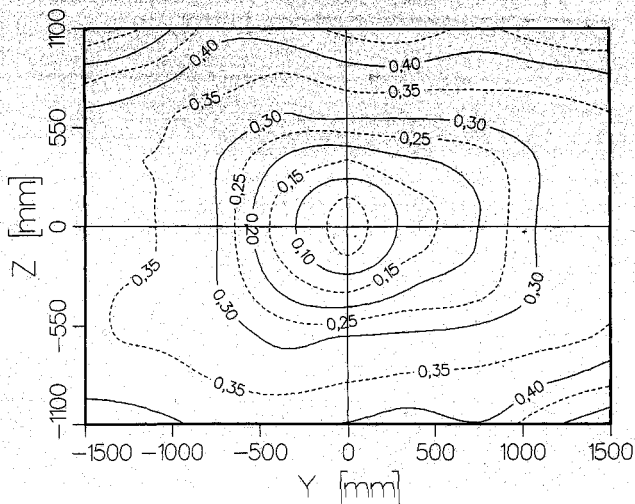


Fig. 9 Axial turbulence level $Tu_x(\%)$ in the test section center at 50 m/s after modernization.

to install a single turbulence screen downstream of the existing honeycomb of the tunnel. The final design of the settling chamber region is indicated in Fig. 6. Immediately downstream ($x/M = 2.9$) of the honeycomb ($L = 600$ mm, $L/M = 8.2$) a single turbulence screen with an open-area ratio of 58% ($M = 2.1$ mm, $d = 0.5$ mm) is installed. Because it is known that soldered seams of screens which are made from several pieces can have negative effects on the turbulence level in the test section,¹² a screen made from a single piece with a cross-sectional area of 4.8×6.8 m² is used.

For honeycomb-screen combinations similar to that described above, Scheiman and Brooks measured an average turbulence reduction factor of $f \approx 0.25$ for the axial turbulence, and a reduction factor of $f_{hc} \approx 0.65$ for the honeycomb alone. With these values, the axial turbulence level to be expected in the closed test section of the modernized tunnel was estimated by using the corresponding contraction ratios and the turbulence level of 0.75%, which was measured at a test section velocity of 50 m/s in the old tunnel configuration, as follows:

$$Tu_{x,new} \approx Tu_{x,old} \cdot \frac{CR_{old}}{CR_{new}} \cdot \frac{f}{f_{hc}}$$

$$= 0.75\% \cdot \frac{4.6}{5.2} \cdot \frac{0.25}{0.65} \approx 0.25\%$$

Therefore, the axial turbulence level of the new tunnel configuration was expected to be in the order of 0.25%. Figure 9 represents the axial turbulence level distribution in the center cross section of the test section measured at 50 m/s after reoperation of the modernized tunnel. The turbulence level increases from 0.05% on the centerline to a value of about 0.45% near the test section walls. This means that the average turbulence level is in fact about 0.25% and shows that the design goals have been fully achieved. Moreover, these values clearly confirm the design of the settling chamber, and therefore, the investigations of Scheiman and Brooks.¹¹

Flow Quality After Modernization of the Tunnel

After reoperation of the modernized tunnel, the test section flowfield was investigated and calibrated extensively. As mentioned earlier, the first measurements of the test section velocity and the corresponding power requirements showed that the tunnel achieves a maximum test section velocity of 70 m/s as was predicted in the design period. This confirms that the predicted fan operating points and fan efficiencies, as well as the predicted power requirements, were absolutely met (Fig. 4).

The measurement of the axial turbulence level (which was already presented in Fig. 9) showed that the new closed test section and the new settling chamber design results in a relatively low turbulence level with an average value of about 0.25% in the test section center compared to a value of 0.75% measured on the centerline of the old tunnel configuration. This means that the turbulence level could be reduced by a factor of 3. However, using the turbulence data measured on centerline of the modified tunnel results in a reduction factor of 15, which indicates that the average reduction factor is even higher than 3.

Figure 10 shows the measured dynamic pressure variations in the center cross section of the test section at a test section velocity of 50 m/s. The lines of constant dynamic pressure variation are concentric to the test section axis and show that the flowfield has become essentially more uniform than in the old tunnel. The maximum variations in dynamic pressure outside the boundary layers are in the order of $\pm 1.0\%$ compared to $\pm 4\%$ of the old tunnel configuration. However, although the dynamic pressure distribution shows an important improvement, the measured variations are higher as theoretically predicted and still not wholly acceptable compared to the flow quality which is normally achieved in modern wind tunnels.

Figure 11 represents a closer look at this problem by showing the dynamic pressure distribution in a three-dimensional graph. Figure 11 clearly reveals that there is a region of low

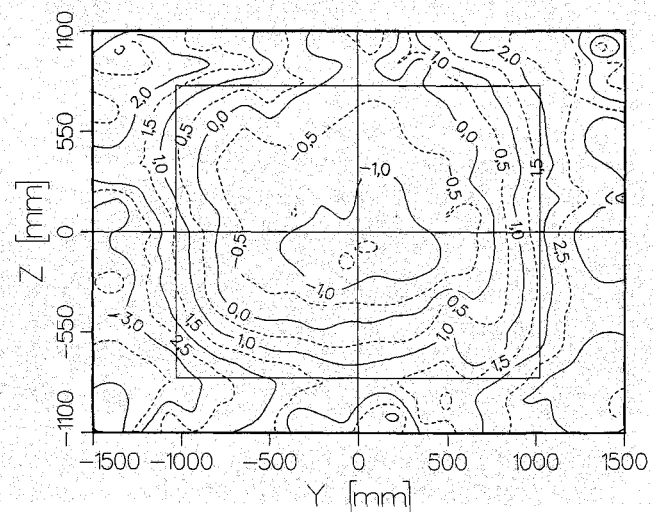


Fig. 10 Dynamic pressure variations from average in (%) at 50 m/s after modernization.

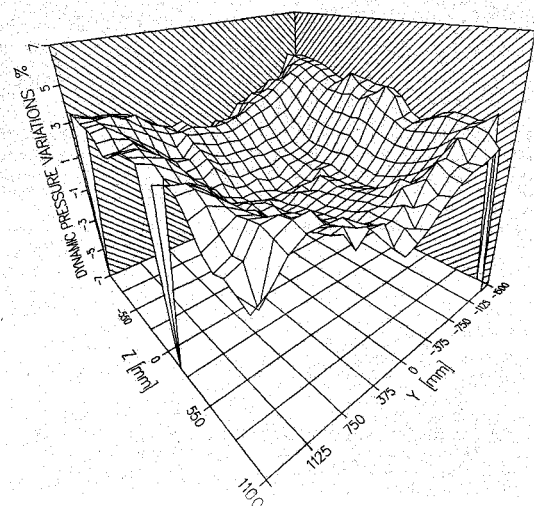


Fig. 11 Three-dimensional representation of the dynamic pressure distribution.

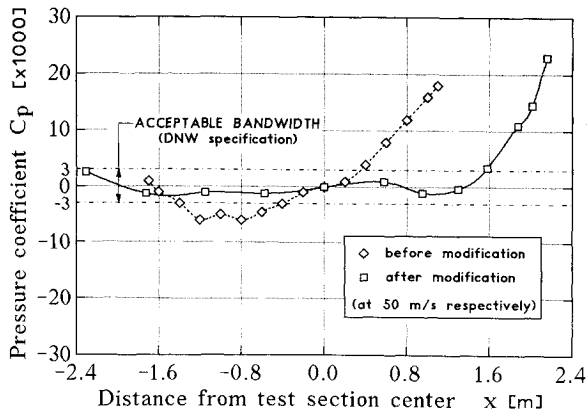


Fig. 12 Comparison of the static pressure distribution on test section centerline before and after modernization.

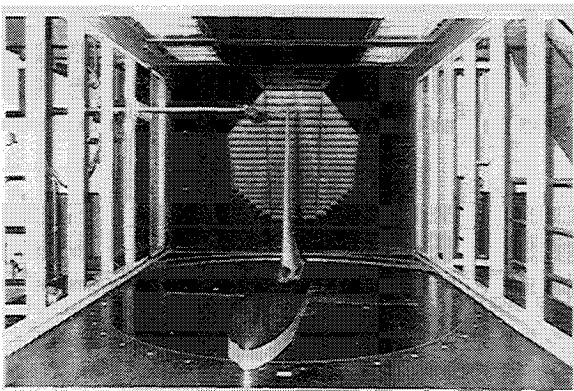


Fig. 13 View downstream through the new closed test section (with mounted A310 half-model).

velocity symmetrical to the test section centerline, and a concentric region of high velocity near the test section walls. Although the calculation of the inviscid flowfield through the contraction showed no similar effects, the reason for this seems to be a contraction-cone overshoot which is possibly produced by the displacement effect of the boundary layers. On the other hand, it is well known that screens itself also produce some over-speeds near the walls.¹³ Therefore, it is mostly recommended to install the last turbulence screen of the settling chamber at least 0.2 hydraulic diameters upstream of the contraction inlet. In the actual case, the screen is installed even somewhat downstream of the contraction inlet. From that point of view, it is also possible that the observed contraction cone overshoot is triggered (or at least intensified) by the turbulence screen. This problem is currently under research.

Figure 12 shows the static pressure distribution along the test section centerline before modernization in comparison to the data measured after modernization of the tunnel. As can be seen, the measured data clearly confirm the selected test section side-wall angle of 0.24 deg and show that the design goal of a maximum pressure variation of $\pm 0.003 \cdot c_p$ is achieved up to 80% of the test section length (the pressure rise at the downstream end of the test section is due to the ventilation to the ambient).

Finally, Fig. 13 shows a downstream view through the new test section with a mounted AIRBUS A 310 half-model. This model was used for the first calibration measurements with the new external balance. The results of these measurements showed an outstanding agreement with the data measured in the nonreturn wind tunnel of Deutsche Airbus, Bremen (Germany), which confirms the qualities of the new external six-component platform balance.

Conclusions

The successful modernization of the low-speed wind tunnel of the Technical University of Darmstadt, Germany, shows that the flow quality of existing wind tunnels which do not represent the state-of-art can be improved essentially by a careful application of the aerodynamic design rules, even if an optimum tunnel design cannot be realized.

Moreover, the modernization project offered the chance to review, apply, and verify today's known aerodynamic design rules of the basic wind-tunnel components. The results show that most of the applied design rules can be confirmed. However, the various unconventional compromises and designs which had to be realized throughout the modernization period show that there is still potential for further improvements and that there is especially a lack of reliable design rules for the design and optimization of very short three-dimensional contractions.

Acknowledgment

This research was supported by the German Ministry for Research and Technology (BMFT) under Contract LVW 850217.

References

- ¹Michel, U., and Froebel, E., "Lower Limit for the Velocity Fluctuations in Wind Tunnels," *Experiments in Fluids*, Vol. 6, No. 1, 1988, pp. 49–54.
- ²Eckert, W. T., Mort, K. W., and Jope, J., "Aerodynamic Design Guidelines and Computer Program for Estimation of Subsonic Wind Tunnel Performance," NASA TN D-8243, Oct. 1976.
- ³Wolf, T., "Estimation of Power Requirements and Investigation for Modification of the University of Darmstadt 3 m Low-Speed Wind Tunnel," (in German), Technical Univ. of Darmstadt, Rept. 42/88, Darmstadt, Germany, April 1988.
- ⁴Wallis, R. A., *Axial Flow Fans, Design and Practice*, 1st ed., George Newnes, London, 1961, p. 162.
- ⁵Boerger, G. G., "The Optimization of Wind Tunnel Contractions for the Subsonic Range," NASA TTF 18899, March 1976.
- ⁶Schilawa, S., "Design of Three-Dimensional Wind Tunnel Contractions," (in German), Fortschrittsbericht der VDI-Zeitschriften, Reihe 7, Nr. 82, VDI-Verlag GmbH, Bochum, Düsseldorf, Germany, 1984.
- ⁷Sanderse, A., "Users-Guide for a Set of Computer Programs Applicable in Design and Analysis of Contraction Contours with Varying Rectangular Cross-Section for Low-Speed Wind Tunnels," National Aerospace Lab. of The Netherlands (NLR), Memorandum IN-83-009 U, April 1983.
- ⁸Klein, A., Ramjee, V., and Venkataramani, K. S., "An Experimental Study of the Subsonic Flow in Axisymmetric Contractions," *Journal of Flight Sciences and Space Research*, Vol. 1, No. 9, 1973, pp. 312–320.
- ⁹Rouse, H., and Hassan M. M., "Cavitation-Free Inlets and Contractions," *Mechanical Engineering*, Vol. 71, No. 3, 1949, pp. 213–216.
- ¹⁰Loehrke, R. I., and Nagib, H. M., "Control of Free-Stream Turbulence by Means of Honeycombs: A Balance Between Suppression and Generation," *Journal of Fluids Engineering*, Vol. 98, Ser. 1, No. 3, 1976, pp. 342–353.
- ¹¹Scheiman, J., and Brooks, J. D., "A Comparison of Experimental and Theoretical Turbulence Reduction from Screens, Honeycomb and Honeycomb-Screen Combinations," AIAA Paper 80-0433, Colorado Springs, CO, March 1980, pp. 129–137.
- ¹²Otto, H., "Influence of Wind Tunnel Circuit Installations on Test Section Flow Quality," International Congress on Instrumentation in Aerospace Simulation Facilities, Deutsche Forschungsanstalt für Luft- und Raumfahrt (DLR), Research Center Göttingen (Germany), IEEE Publication 89CH2762-3, Sept. 18–21, 1989.
- ¹³Mehta, R. D., "Turbulent Flow Through Screens," AIAA Paper 84-0538, Reno, NV, Jan. 1984.